EXTENDED PDF FORMAT
SPONSORED BY
usb
Products from Affymetrix
www.usbweb.com

Disruption of the CFTR Gene Produces a Model of Cystic Fibrosis in Newborn Pigs

Christopher S. Rogers, *et al.*

Science **321**, 1837 (2008);
DOI: 10.1126/science.1163600

The following resources related to this article are available online at www.sciencemag.org (this information is current as of November 6, 2008):

Updated information and services, including high-resolution figures, can be found in the online version of this article at:
http://www.sciencemag.org/cgi/content/full/321/5897/1837

Supporting Online Material can be found at:
http://www.sciencemag.org/cgi/content/full/321/5897/1837/DC1

A list of selected additional articles on the Science Web sites **related to this article** can be found at:
http://www.sciencemag.org/cgi/content/full/321/5897/1837#related-content

This article **cites 26 articles**, 10 of which can be accessed for free:
http://www.sciencemag.org/cgi/content/full/321/5897/1837#otherarticles

This article appears in the following **subject collections**:
Medicine, Diseases
http://www.sciencemag.org/cgi/collection/medicine

Information about obtaining **reprints** of this article or about obtaining **permission to reproduce this article** in whole or in part can be found at:
http://www.sciencemag.org/about/permissions.dtl

Downloaded from www.sciencemag.org on November 6, 2008

Science (print ISSN 0036-8075; online ISSN 1095-9203) is published weekly, except the last week in December, by the American Association for the Advancement of Science, 1200 New York Avenue NW, Washington, DC 20005. Copyright 2008 by the American Association for the Advancement of Science; all rights reserved. The title *Science* is a registered trademark of AAAS.

antigens. Because we do not yet have sufficient VLR and TLR complex structures to make statistically significant conclusions, and the number of LRR modules in TLRs is much greater than in VLRs, it may be too early to infer evolutionary relationships between VLRs and TLRs.

The crystal structure of RBC36-ECD in complex with the H-trisaccharide has provided structural insight into how VLRs recognize their antigens and provides a basis for rational design and modification of other antigen-specific VLRs. This VLR-antigen structure sheds light on the adaptation and evolution of primordial LRR proteins into their more specialized roles in pathogen recognition (e.g., TLRs) by the mammalian innate immune system.

References and Notes

1. Z. Pancer *et al.*, *Nature* **430**, 174 (2004).
2. M. N. Alder *et al.*, *Science* **310**, 1970 (2005).
3. When the distribution of LRRV modules per transcript was analyzed from 517 unique VLR sequences, VLRs were found to have an average of 1.31 LRRV modules between the canonical LRR1 and LRRVe modules (*2*): 109 VLRs (0 LRRV), 228 VLRs (1 LRRV), 119 VLRs (2 LRRVs), 45 VLRs (3 LRRVs), 6 VLRs (4 LRRVs), 8 VLRs (5 LRRVs), 1 VLR (6 LRRVs), and 1 VLR (7 LRRVs).
4. Z. Pancer *et al.*, *Proc. Natl. Acad. Sci. U.S.A.* **102**, 9224 (2005).
5. J. Choe, M. S. Kelker, I. A. Wilson, *Science* **309**, 581 (2005); published online 16 June 2005 (10.1126/science.1115253).
6. J. K. Bell *et al.*, *Proc. Natl. Acad. Sci. U.S.A.* **102**, 10976 (2005).
7. H. M. Kim *et al.*, *J. Biol. Chem.* **282**, 6726 (2007).
8. B. R. Herrin *et al.*, *Proc. Natl. Acad. Sci. U.S.A.* **105**, 2040 (2008).
9. M. N. Alder *et al.*, *Nat. Immunol.* **9**, 319 (2008).
10. G. A. Boffa, J. M. Fine, A. Drilhon, P. Amouch, *Nature* **214**, 700 (1967).
11. B. Pollara, G. W. Litman, J. Finstad, J. Howell, R. A. Good, *J. Immunol.* **105**, 738 (1970).
12. At least four subtypes of H-antigens are known, which can be further converted into the A-antigen of human blood group A and B-antigen of human blood group B by glycosyltransferases A and B, respectively (*31*) (fig. S1).
13. See supporting material on *Science* Online.
14. Single-letter abbreviations for amino acid residues: A, Ala; C, Cys; D, Asp; E, Glu; F, Phe; G, Gly; H, His; I, Ile; K, Lys; L, Leu; M, Met; N, Asn; P, Pro; Q, Gln; R, Arg; S, Ser; T, Thr; V, Val; W, Trp; Y, Tyr.
15. S. F. Altschul *et al.*, *Nucleic Acids Res.* **25**, 3389 (1997).
16. S. Sheriff, W. A. Hendrickson, J. L. Smith, *J. Mol. Biol.* **197**, 273 (1987).
17. B. R. Gelin, M. Karplus, *Biochemistry* **18**, 1256 (1979).
18. M. L. Connolly, *J. Mol. Graph.* **11**, 139 (1993).
19. I. A. Wilson, R. L. Stanfield, *Curr. Opin. Struct. Biol.* **3**, 113 (1993).
20. Aromatic residues, such as Trp and Tyr, are frequently observed in the protein sugar-binding sites. For example, in the maltose/maltooligosaccharide-binding protein (*32*), aromatic residues play a major role in carbohydrate recognition and binding by providing not only hydrophobic stacking interactions between aromatic residues and the hydrophobic face of the sugar rings, but also polar contacts to the sugar hydroxyl groups.
21. I. B. Rogozin *et al.*, *Nat. Immunol.* **8**, 647 (2007).
22. E. G. Huizinga *et al.*, *Science* **297**, 1176 (2002).
23. L. Holm, C. Sander, *J. Mol. Biol.* **233**, 123 (1993).
24. I. A. Wilson, R. L. Stanfield, *Curr. Opin. Struct. Biol.* **4**, 857 (1994).
25. K. C. Garcia, L. Teyton, I. A. Wilson, *Annu. Rev. Immunol.* **17**, 369 (1999).
26. P. von Gara, *Z. Immunitaetsforsch. Exp. Ther.* **71**, 1 (1931).
27. T. T. Wu, G. Johnson, E. A. Kabat, *Proteins* **16**, 1 (1993).
28. H. M. Kim *et al.*, *Cell* **130**, 906 (2007).
29. M. S. Jin *et al.*, *Cell* **130**, 1071 (2007).
30. L. Liu *et al.*, *Science* **320**, 379 (2008).
31. F. Yamamoto, P. D. McNeill, S. Hakomori, *Biochem. Biophys. Res. Commun.* **187**, 366 (1992).
32. X. Duan, F. A. Quiocho, *Biochemistry* **41**, 706 (2002).
33. Molecular Operating Environment (MOE), version 2000.09 (Chemical Computing Group, Montreal, 2003).

34. We thank R. L. Stanfield, X. Dai, and X. Zhu for help with data collection and analysis; M. N. Alder for help with VLR cDNA library preparation; J. Paulson and R. McBride for helpful comments and suggestions; and J. Vanhnasy, B. Droese, and H.-J. Kim for technical support and advice. Portions of this research were carried out at the Stanford Synchrotron Radiation Laboratory (SSRL), operated by Stanford University on behalf of the U.S. Department of Energy, Office of Basic Energy Sciences. Supported by NIH grants AI42266 (I.A.W.) and AI072435 (M.D.C.), the Georgia Research Alliance (M.D.C.), and the Skaggs Institute for Chemical Biology (I.A.W.). This is Scripps Research Institute manuscript 19581-MB. Coordinates and structure factors have been deposited in the Protein Data Bank (PDB) with accession code 3E6J.

Supporting Online Material

www.sciencemag.org/cgi/content/full/321/5897/1834/DC1
Materials and Methods
Figs. S1 to S4
Tables S1 to S2
References

30 June 2008; accepted 28 August 2008
10.1126/science.1162484

Disruption of the *CFTR* Gene Produces a Model of Cystic Fibrosis in Newborn Pigs

Christopher S. Rogers,[1]* David A. Stoltz,[1]* David K. Meyerholz,[2]* Lynda S. Ostedgaard,[1] Tatiana Rokhlina,[1] Peter J. Taft,[1] Mark P. Rogan,[1] Alejandro A. Pezzulo,[1] Philip H. Karp,[1,3] Omar A. Itani,[1] Amanda C. Kabel,[1] Christine L. Wohlford-Lenane,[4] Greg J. Davis,[1] Robert A. Hanfland,[5] Tony L. Smith,[5] Melissa Samuel,[6] David Wax,[6] Clifton N. Murphy,[6] August Rieke,[6] Kristin Whitworth,[6] Aliye Uc,[4] Timothy D. Starner,[4] Kim A. Brogden,[7] Joel Shilyansky,[5] Paul B. McCray Jr.,[4] Joseph Zabner,[1] Randall S. Prather,[6] Michael J. Welsh[1,3,8]†

Almost two decades after *CFTR* was identified as the gene responsible for cystic fibrosis (CF), we still lack answers to many questions about the pathogenesis of the disease, and it remains incurable. Mice with a disrupted *CFTR* gene have greatly facilitated CF studies, but the mutant mice do not develop the characteristic manifestations of human CF, including abnormalities of the pancreas, lung, intestine, liver, and other organs. Because pigs share many anatomical and physiological features with humans, we generated pigs with a targeted disruption of both *CFTR* alleles. Newborn pigs lacking CFTR exhibited defective chloride transport and developed meconium ileus, exocrine pancreatic destruction, and focal biliary cirrhosis, replicating abnormalities seen in newborn humans with CF. The pig model may provide opportunities to address persistent questions about CF pathogenesis and accelerate discovery of strategies for prevention and treatment.

Understanding human disease often requires the use of animal models. Mice have been the overwhelming species of choice because methods for specifically altering their genome have been readily available. However, in many cases, mice with targeted gene manipulations fail to replicate phenotypes observed in humans—one example is cystic fibrosis (CF).

In 1938, Dorothy Andersen coined the term "cystic fibrosis of the pancreas" (*1*). Over the ensuing years, investigators learned that CF involved many other organs, including the intestine, lung, sweat gland, liver, gallbladder, and male genital tract (*2*–*4*). We now know CF to be a common, autosomal recessive disease with a carrier rate of ~5% in Caucasians. In 1989, the gene mutated in CF was identified, and its product was named cystic fibrosis transmembrane conductance regulator (CFTR) (*5*). Soon thereafter, it was discovered that CFTR is a regulated anion channel that may also affect other transport processes (*3*).

Despite many advances, our understanding of CF pathogenesis remains incomplete, thus hindering the development of new therapies. This begs the question: Why have we not made more progress? Whereas superb clinical research has guided thoughts about CF, interpretations about pathogenesis are often based on observations ob-

[1]Department of Internal Medicine, Roy J. and Lucille A. Carver College of Medicine, University of Iowa, Iowa City, IA 52242, USA. [2]Department of Pathology, Roy J. and Lucille A. Carver College of Medicine, University of Iowa, Iowa City, IA 52242, USA. [3]Howard Hughes Medical Institute (HHMI), Roy J. and Lucille A. Carver College of Medicine, University of Iowa, Iowa City, IA 52242, USA. [4]Department of Pediatrics, Roy J. and Lucille A. Carver College of Medicine, University of Iowa, Iowa City, IA 52242, USA. [5]Department of Surgery, Roy J. and Lucille A. Carver College of Medicine, University of Iowa, Iowa City, IA 52242, USA. [6]Division of Animal Sciences, University of Missouri, Columbia, MO 65211, USA. [7]Department of Periodontics and Dows Institute for Dental Research, College of Dentistry, University of Iowa, Iowa City, IA 52242, USA. [8]Department of Molecular Physiology and Biophysics, Roy J. and Lucille A. Carver College of Medicine, University of Iowa, Iowa City, IA 52242, USA.

*These authors contributed equally to this work.
†To whom correspondence should be addressed. E-mail: michael-welsh@uiowa.edu

Downloaded from www.sciencemag.org on November 6, 2008

tained long after the disease onset, and many studies cannot be carried out in humans. Cell-based models have also proven valuable for research (*6*) but are limited because the disease involves a whole organism. Gene-targeted mouse models have likewise been instructive about CF, yet the mutant mice do not develop the pancreatic, airway, intestinal, or liver disease typically found in humans (*7*–*9*).

To develop a new CF model, we chose pigs because in terms of anatomy, biochemistry, physiology, size, life span, and genetics, they are more similar to humans than are mice (*10*, *11*). We used homologous recombination in fibroblasts of outbred domestic pigs to disrupt the *CFTR* gene and somatic cell nuclear transfer to generate $CFTR^{+/-}$ pigs (*12*).

At sexual maturity (~6 to 7 months), female $CFTR^{+/-}$ pigs were bred to $CFTR^{+/-}$ males. Six litters produced 64 piglets. Genotyping (Fig. 1A) revealed 18 $CFTR^{+/+}$, 26 $CFTR^{+/-}$, and 20 $CFTR^{-/-}$ animals, a ratio not significantly different from the expected ratio of 1:2:1 (*13*). Figure 1B shows the first litter. Birth weights varied but did not segregate by genotype (Fig. 1C). The piglets looked normal at birth, and their genotype could not be discerned by appearance. A normal appearance is consistent with findings in humans.

Northern blot analysis and quantitative reverse transcription polymerase chain reaction (RT-PCR) did not detect normal *CFTR* transcripts (Fig. 1A). Immunoprecipitation detected no normal CFTR protein. Like human CFTR (*14*, *15*), in wild-type (WT) tissue the porcine protein localized apically in airway epithelia and ileal crypts (Fig. 1D).

We assessed CFTR function in vivo by measuring transepithelial voltage (Vt) across nasal epithelia (*16*) (Fig. 1, E and F). As in humans with CF, baseline Vt was hyperpolarized in $CFTR^{-/-}$ piglets. Amiloride, which inhibits ENaC Na^+ channels, reduced Vt in all genotypes. To test for CFTR channel activity, we perfused the apical surface with a Cl^--free solution and added isoproterenol to increase cellular levels of cyclic adenosine monophosphate; these interventions hyperpolarized nasal Vt in WT and heterozygous pigs, but not $CFTR^{-/-}$ animals. Perfusion with adenosine triphosphate to activate P2Y2 receptors and Ca^{2+}-activated Cl^- channels (*17*) further hyperpolarized Vt, and the response did not differ significantly

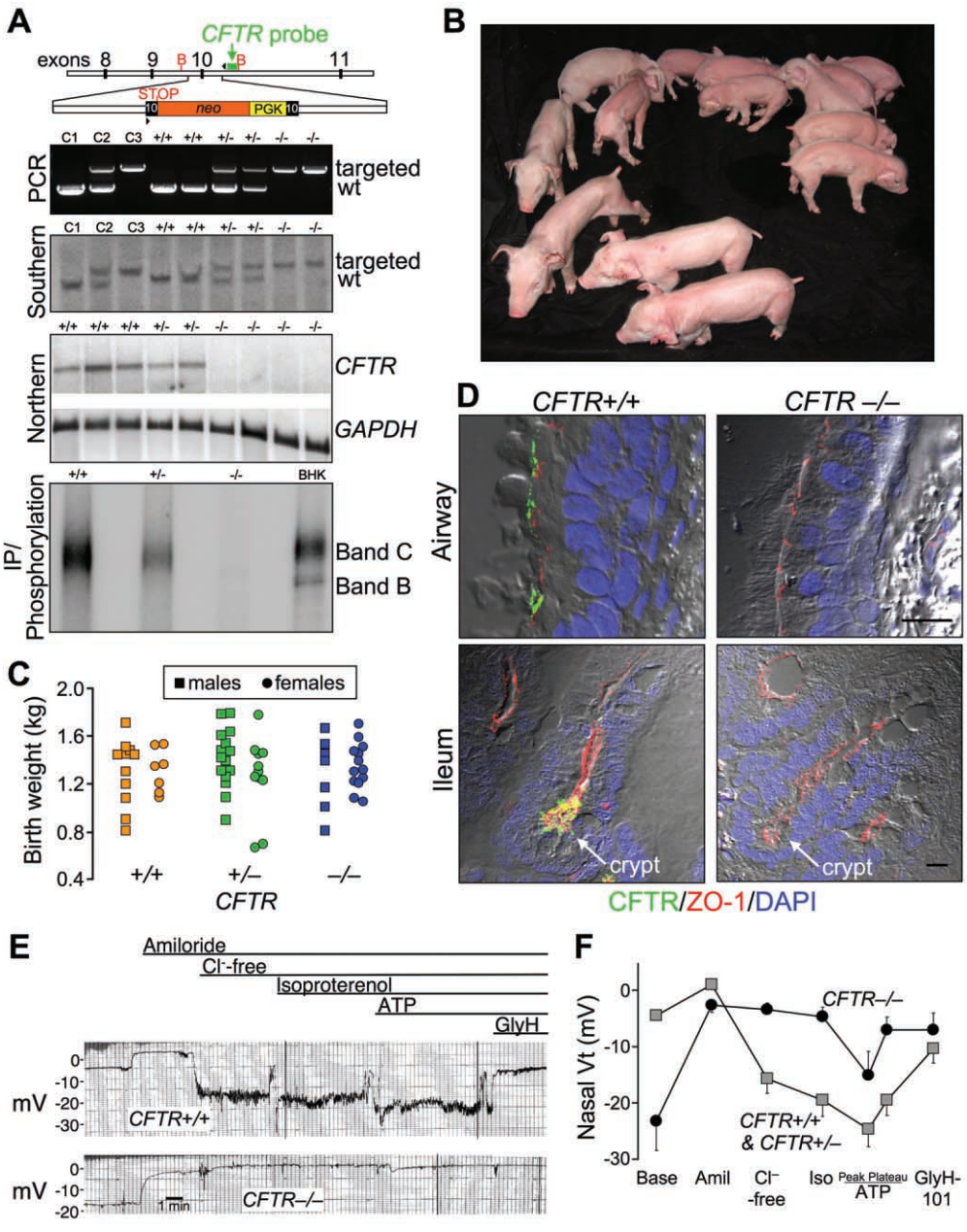

Fig. 1. $CFTR^{-/-}$ piglets appear normal at birth. (**A**) Upper panel depicts insertion into porcine *CFTR* exon 10 of a phosphoglycerate kinase (PGK) promoter (yellow) driving a neomycin resistance cDNA (orange), and an engineered stop codon. Position of probe (green), PCR primers (arrowheads), and *Bgl*II sites (B) is indicated. The second and third panels show genotyping by PCR and Southern blot analysis of genomic DNA. Lanes C1, C2, and C3 contain controls of $CFTR^{+/+}$, $^{+/-}$, and $^{-/-}$ DNA, respectively. The fourth panel shows Northern blot analysis of ileal *CFTR* and *GAPDH* mRNA. Consistent with the Northern blot, quantitative RT-PCR of exon 10 (the targeted site) detected <0.1% of *CFTR* transcripts in $CFTR^{-/-}$ ileum, relative to $CFTR^{+/+}$ (n = 6 and 4 piglets, respectively). The bottom panel shows immunoprecipitation (IP) and phosphorylation of CFTR plus recombinant CFTR in baby hamster kidney cells. (**B**) First litter containing piglets of all three genotypes. (**C**) Birth weights. Mean ± SD of weights: 1.31 ± 0.24 kg for $CFTR^{+/+}$ (orange), 1.35 ± 0.28 kg for $CFTR^{+/-}$ (green), and 1.31 ± 0.23 kg for $CFTR^{-/-}$ (blue) animals. (**D**) Immunocytochemistry of CFTR in airway epithelia (top) and ileum (bottom). Figures are differential interference contrast with staining for ZO-1 (a component of tight junctions, red), CFTR (green), and nuclei (4′,6′-diamidino-2-phenylindole, blue). See also fig. S1. Scale bars, 10 μm. (**E**) Tracings of in vivo nasal Vt measured in newborn pigs. After baseline measurements, the following agents/solutions were sequentially added to the epithelial perfusate: amiloride (100 μM), Cl^--free solution, isoproterenol (10 μM), ATP (100 μM), and GlyH-101 (100 μM). (**F**) Average nasal Vt measurements as indicated in (E). Data from four $CFTR^{+/+}$ and four $CFTR^{+/-}$ piglets (gray squares) were not statistically different and were combined and compared with data from five $CFTR^{-/-}$ piglets (blue circles). Values of baseline nasal Vt for $CFTR^{-/-}$ piglets differed from the controls, as did the changes in Vt induced by adding amiloride, a Cl^--free solution, and GlyH-101 (all $P < 0.05$). Data are mean ± SEM.

Downloaded from www.sciencemag.org on November 6, 2008

between genotypes. Perfusion with the CFTR inhibitor GlyH-101 (*18*) depolarized Vt in controls animals, but not in *CFTR*$^{-/-}$ piglets. These data reveal the loss of CFTR Cl^- channel activity in newborn *CFTR*$^{-/-}$ pigs. Whereas the lack of data from newborn humans precludes a direct comparison, our data qualitatively match those from adults and children with CF (*16*).

What phenotypes would be expected if newborn *CFTR*$^{-/-}$ piglets model human disease? Figure 2A shows some human CF phenotypes and the time spans when they become clinically apparent (*3*, *19*). The earliest manifestation (hours to 2 days) is meconium ileus, an intestinal obstruction occurring in ~15% of CF infants (*2*, *3*, *19*, *20*). Obstruction can occur throughout the small intestine or colon, but it is most often observed near the ileocecal junction. Distal to the obstruction, the bowel is small and atretic (microcolon). Intestinal perforation in utero or postnatally occurs in some infants.

Newborn *CFTR*$^{-/-}$ piglets failed to pass feces or gain weight (Fig. 2B). By 24 to 40 hours of age, they stopped eating, developed abdominal distension, and had bile-stained emesis, which are clinical signs of intestinal obstruction. We examined histopathology between birth and 12 hours in piglets that had not eaten and between 24 and 40 hours in piglets that were fed colostrum and milk replacer. Except as noted, the pathologic changes refer to the earlier time period. After 30 to 40 hours, the stomachs of *CFTR*$^{-/-}$ piglets contained small amounts of green, bile-stained milk (Fig. 2C). The proximal small intestine was dilated by small amounts of milk and abundant gas. The site of obstruction ranged from mid-distal small intestine to proximal spiral colon, the anatomical equivalent of the human ascending colon. Perforation and peritonitis occurred in some piglets. Dark green meconium distended the *CFTR*$^{-/-}$ intestine, and adjacent villi showed degeneration and atrophy, whereas *CFTR*$^{+/+}$ ileum had long villi (Fig. 2D). Distal to the meconium, luminal diameter was reduced with mild-to-severe mucinous hyperplasia, including mucoid luminal "plugs" (Fig. 2E). These changes replicate those seen in humans with CF (*3*, *19*).

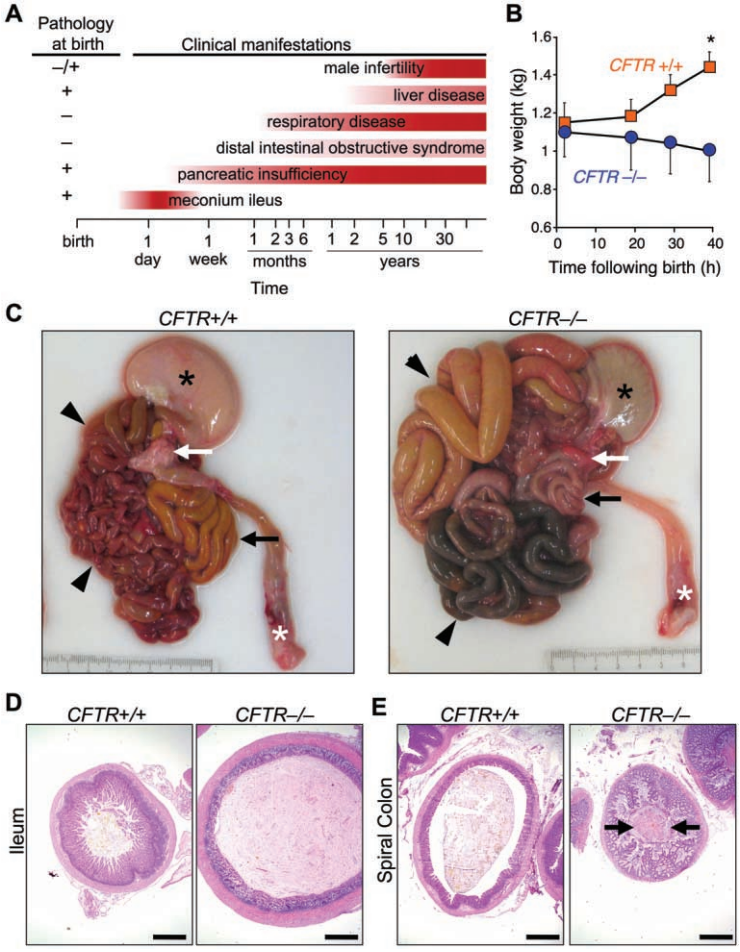

Fig. 2. *CFTR*$^{-/-}$ piglets develop meconium ileus. (**A**) Schematic shows some clinical and histopathological CF manifestations. Pathological abnormalities are present before clinical disease becomes apparent. (**B**) Weight after birth. Animals were fed colostrum and milk-replacer. $n = 7$ *CFTR*$^{+/+}$ and 4 *CFTR*$^{-/-}$ piglets. Data are mean ± SEM. $^*P < 0.05$. (**C**) Gross appearance of gastrointestinal tract. Piglets were fed colostrum and milk-replacer for 30 to 40 hours and then euthanized. Stomach, black asterisk; small intestine, arrowheads; pancreas, white arrow; rectum, white asterisk; and spiral colon, black arrow. Of 16 *CFTR*$^{-/-}$ piglets, the obstruction occurred in the small intestine in 7 animals and in spiral colon in 9. (**D** and **E**) Microscopic appearance of the ileum (D) and colon (E). Hematoxylin and eosin (H&E) stain. Scale bars, 1 mm. Images are representative of severe meconium ileus occurring in 16 out of 16 (16/16) *CFTR*$^{-/-}$ piglets.

The penetrance of meconium ileus was 100% in *CFTR*$^{-/-}$ piglets versus ~15% in human CF. Potential explanations for this difference include a restricted genetic background in our pig model versus that in humans, a null mutation in the pigs versus mutations in humans that might yield tiny amounts of protein function, and anatomical or physiological differences [see footnote F1 in (*13*)].

Exocrine pancreatic insufficiency afflicts 90 to 95% of patients with CF (*1*–*4*, *19*, *21*, *22*). The porcine *CFTR*$^{-/-}$ pancreas was small (Fig. 3A), and microscopic examination revealed small, degenerative lobules with increased loose adipose and myxomatous tissue, as well as scattered-to-moderate cellular inflammation (Fig. 3, B and C). Residual acini had diminished amounts of eosinophilic zymogen granules (Fig. 3D). Centroacinar spaces, ductules, and ducts were variably dilated and obstructed by eosinophilic material plus infrequent neutrophils and macrophages mixed with cellular debris (Fig. 3E). Ducts and ductules had foci of mucinous metaplasia. Pancreatic endocrine tissue was spared (Fig. 3C). These changes are similar to those originally described by Andersen and others (*1*, *19*, *21*) in their studies of human CF.

Humans often require surgery to relieve meconium ileus (*3*). We performed an ileostomy on one *CFTR*$^{+/+}$ piglet and three *CFTR*$^{-/-}$ piglets. Because of technical problems in postoperative care, only one piglet (genotype *CFTR*$^{-/-}$) out of the four recovered. Once newborn infants recover from meconium ileus, the course of their disease resembles that in other patients. Likewise, the piglet grew and went on to develop pancreatic insufficiency. At 10 weeks, the piglet had an episode resembling "distal intestinal obstruction syndrome," which was successfully treated as in humans (*3*) [also see footnote F2 in (*13*)]. Although these observations were based on a single animal, they bore a marked resemblance to clinical observations of human CF.

Focal biliary cirrhosis is the second most common cause of CF mortality (*3*, *20*, *23*). The porcine *CFTR*$^{-/-}$ liver revealed infrequent, mild-to-moderate hepatic lesions (Fig. 3F). Chronic cellular inflammation, ductular hyperplasia, and mild fibrosis were typical of focal biliary cirrhosis. Gallbladder abnormalities, including gallstones, occur in 15 to 30% of patients, and a small gallbladder is a common autopsy finding (*3*). Similarly, porcine *CFTR*$^{-/-}$ gallbladders were small and often filled with congealed bile and mucus (Fig. 3, G and H). Epithelia showed diffuse mucinous changes with folds extending into the lumen.

Approximately 97% of males with CF are infertile (*3*); the vas deferens is often normal at birth, and obstruction is thought to cause progressive deterioration [see footnote F3 in (*13*)]. In all piglets, the vas deferens appeared to be intact. Paranasal sinus abnormalities occur in most chil-

Downloaded from www.sciencemag.org on November 6, 2008

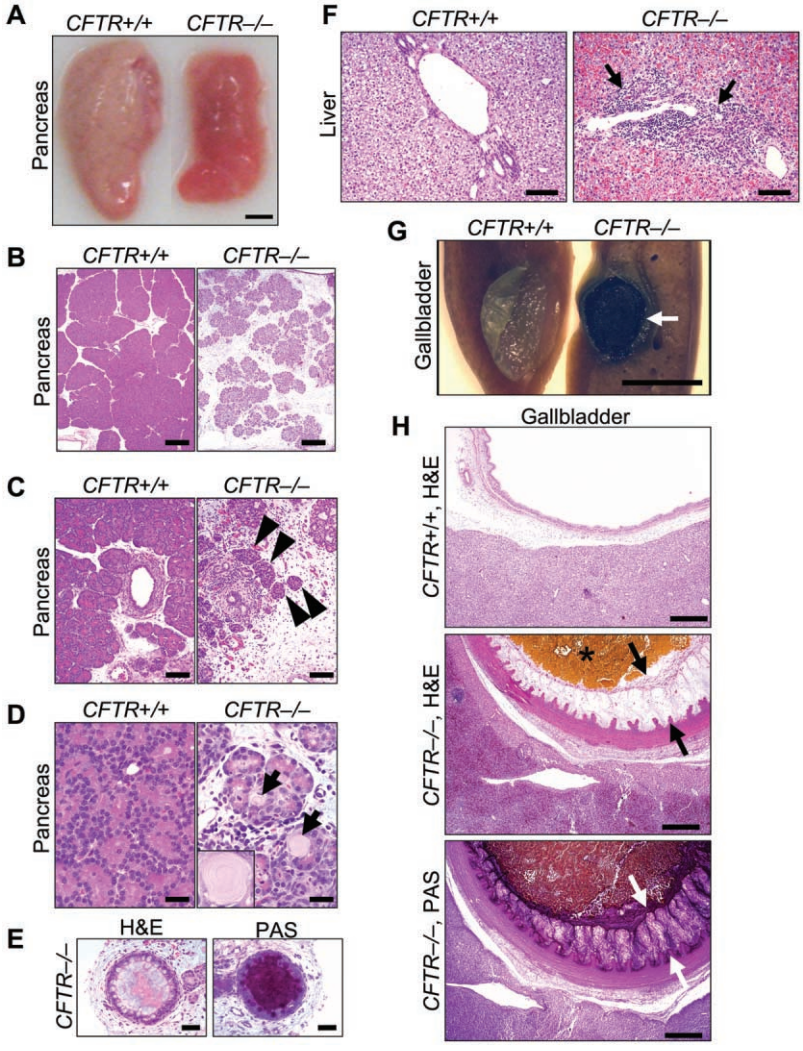

Fig. 3. *CFTR*$^{-/-}$ piglets have exocrine pancreatic destruction and liver and gallbladder abnormalities. (**A**) Gross appearance of pancreas. Scale bar, 0.5 cm. (**B**) Loss of parenchyma in the *CFTR*$^{-/-}$ pancreas. H&E stain. Scale bars, 500 μm. (**C**) Pancreatic ducts and islets of Langerhans (arrowheads). Scale bars, 100 μm. (**D**) *CFTR*$^{-/-}$ ductules and acini dilated by eosinophilic inspissated material that formed concentrically lamellar concretions (arrows and inset). H&E stain. Scale bars, 33 μm. (**E**) Ducts within the *CFTR*$^{-/-}$ pancreas. H&E stain, left; periodic acid–Schiff (PAS) stain, right. Scale bars, 50 μm. (**F**) Microscopic appearance of liver. H&E stain. Arrows indicate focal expansion of portal areas by chronic cellular inflammation. Scale bars, 100 μm. (**G**) Gross appearance of gallbladder. When the *CFTR*$^{+/+}$ gallbladder was sectioned, bile drained away rapidly with collapse of the mucosal wall. *CFTR*$^{-/-}$ bile was congealed (arrow) and retained in the lumen of a smaller gallbladder. Scale bar, 0.5 cm. (**H**) Microscopic appearance of gallbladder. *CFTR*$^{-/-}$ gallbladders had congealed, inspissated bile (asterisk) with variable mucus production (arrows, H&E stain) highlighted as a magenta color in PAS stained tissue. Scale bars, 500 μm. Images are representative of severe pancreatic lesions (15/15 *CFTR*$^{-/-}$ piglets), mild-to-moderate liver lesions (3/15), and mild-to-severe gallbladder/duct lesions (15/15).

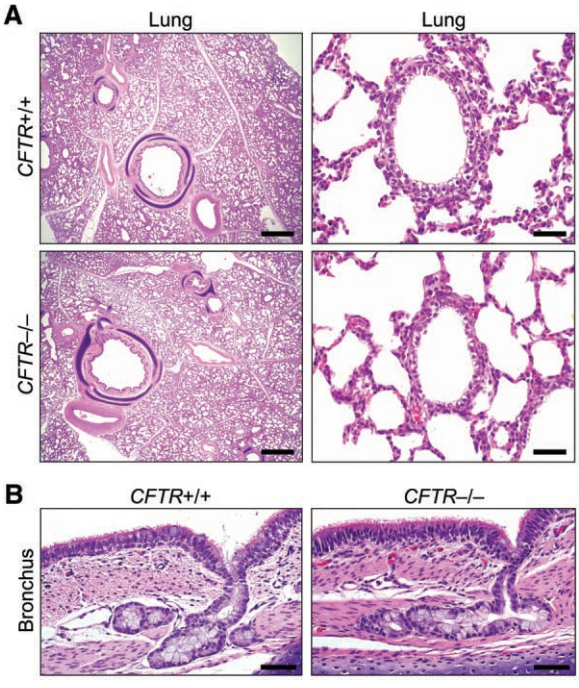

Fig. 4. The lungs of newborn *CFTR*$^{-/-}$ and *CFTR*$^{+/+}$ piglets appear normal. (**A**) Microscopic appearance of lung from piglets <12 hours old. H&E staining. Scale bars, 1 mm (left) and 50 μm (right). (**B**) Bronchial epithelia and submucosal glands. H&E staining. Scale bars, 50 μm. Images are representative of the lack of lesions in 15 out of 15 *CFTR*$^{-/-}$.

dren and adults with CF (*3*). Although *CFTR*$^{-/-}$ porcine paranasal sinuses showed no abnormalities, this negative result is difficult to interpret because it is unclear when sinus disease develops in humans. The salivary glands, nasal cavity, esophageal glands, kidney, heart, striated muscle, spleen, adrenals, eyes, brain, skin, and eccrine sweat glands on the snout revealed no abnormalities in *CFTR*$^{-/-}$ piglets. In all tissues, we observed no differences between WT and heterozygous *CFTR*$^{+/-}$ animals.

Lung disease is the major cause of CF morbidity and mortality (*2*–*4*). The onset of clinical respiratory manifestations varies, with some patients developing symptoms a few months after birth and others after several years. Eventually, most patients develop chronic airway infection and inflammation that destroy the lung. The lungs of neonatal *CFTR*$^{-/-}$ piglets appeared similar to those of their WT littermates. *CFTR*$^{-/-}$ lungs lacked evidence of cellular inflammation in airways or parenchyma (Fig. 4A). Airway epithelia and submucosal glands appeared similar in all three genotypes, and we found no evidence of dilated or plugged submucosal gland ducts [see footnote F4 in (*13*)] (Fig. 4B). Bronchoalveolar lavage 6 to

Downloaded from www.sciencemag.org on November 6, 2008

12 hours after birth showed no evidence of infection, and there were no significant differences between cell counts or levels of interleukin-8 (IL-8) across genotypes (figs. S2 and S3) (*13*).

Whether airway inflammation precedes infection in CF patients or vice versa has been a persistent question. Studies of bronchoalveolar lavage in infants and young children have both supported and argued against the presence of inflammation (increased IL-8 and neutrophilia) without infection (*24*, *25*). In vitro airway epithelial models have also given conflicting results (*26*, *27*). Studies of human fetal trachea transplanted into mice suggested inflammation might occur in developing CF airways (*28*). Although our data do not resolve this controversy, we had the advantage of studying lungs between birth and 12 hours of age, and we found no evidence of abnormal infection or inflammation. Tracking the lungs as $CFTR^{-/-}$ piglets are exposed to additional environmental challenges may inform our understanding of how respiratory disease develops in children and young adults.

The clinical, electrophysiological, and pathological findings in newborn $CFTR^{-/-}$ pigs were markedly similar to those in human neonates with CF (table S1) (*13*). Abdominal lesions dominate the initial presentation in both, with identical appearance of meconium ileus and exocrine pancreatic destruction. In addition, as in humans, the piglets have hepatic changes consistent with early focal biliary cirrhosis and abnormalities of the gallbladder and bile ducts. The lack of abnormalities in the vas deferens and lungs at birth is another similarity. Overall, these encouraging results suggest that the pig model may provide investigators with further opportunities to study CF and develop strategies for prevention and treatment.

References and Notes

1. D. H. Andersen, *Am. J. Dis. Child.* **56**, 344 (1938).
2. P. M. Quinton, *Physiol. Rev.* **79**, S3 (1999).
3. M. J. Welsh, B. W. Ramsey, F. Accurso, G. R. Cutting, in *The Metabolic and Molecular Basis of Inherited Disease*, C. R. Scriver *et al.*, Eds. (McGraw-Hill, New York, 2001), pp. 5121–5189.
4. S. M. Rowe, S. Miller, E. J. Sorscher, *N. Engl. J. Med.* **352**, 1992 (2005).
5. J. R. Riordan *et al.*, *Science* **245**, 1066 (1989).
6. P. H. Karp *et al.*, in vol. 188 of *Epithelial Cell Culture Protocols*, C. Wise, Ed. (Humana, Totowa, NJ, 2002), pp. 115–137.
7. B. R. Grubb, R. C. Boucher, *Physiol. Rev.* **79**, S193 (1999).
8. C. Guilbault, Z. Saeed, G. P. Downey, D. Radzioch, *Am. J. Respir. Cell Mol. Biol.* **36**, 1 (2007).
9. L. L. Clarke, L. R. Gawenis, C. L. Franklin, M. C. Harline, *Lab. Anim. Sci.* **46**, 612 (1996).
10. Z. Ibrahim *et al.*, *Xenotransplantation* **13**, 488 (2006).
11. C. S. Rogers *et al.*, *Am. J. Physiol. Lung Cell Mol. Physiol.* **295**, L240 (2008).
12. C. S. Rogers *et al.*, *J. Clin. Invest.* **118**, 1571 (2008).
13. Supporting material is available on *Science* Online.
14. I. Crawford *et al.*, *Proc. Natl. Acad. Sci. U.S.A.* **88**, 9262 (1991).
15. G. M. Denning, L. S. Ostedgaard, S. H. Cheng, A. E. Smith, M. J. Welsh, *J. Clin. Invest.* **89**, 339 (1992).
16. T. A. Standaert *et al.*, *Pediatr. Pulmonol.* **37**, 385 (2004).
17. S. J. Mason, A. M. Paradiso, R. C. Boucher, *Br. J. Pharmacol.* **103**, 1649 (1991).
18. C. Muanprasat *et al.*, *J. Gen. Physiol.* **124**, 125 (2004).
19. E. H. Oppenheimer, J. R. Esterly, *Perspect. Pediatr. Pathol.* **2**, 241 (1975).
20. M. Wilschanski, P. R. Durie, *J. R. Soc. Med.* **91**, 40 (1998).
21. J. R. Imrie, D. G. Fagan, J. M. Sturgess, *Am. J. Pathol.* **95**, 697 (1979).
22. S. M. Blackman *et al.*, *Gastroenterology* **131**, 1030 (2006).
23. E. H. Oppenheimer, J. R. Esterly, *J. Pediatr.* **86**, 683 (1975).
24. T. Z. Khan *et al.*, *Am. J. Respir. Crit. Care Med.* **151**, 1075 (1995).
25. D. S. Armstrong *et al.*, *Pediatr. Pulmonol.* **40**, 500 (2005).
26. A. A. Stecenko *et al.*, *Inflammation* **25**, 145 (2001).
27. N. Aldallal *et al.*, *Am. J. Respir. Crit. Care Med.* **166**, 1248 (2002).
28. R. Tirouvanziam *et al.*, *Am. J. Respir. Cell Mol. Biol.* **23**, 121 (2000).

29. We thank A. Arias, E. Bagnall, J. Bartlett, B. Bauer, T. Bohnert, E. Burnight, K. Dobbs, C. Dohrn, L. Dowell, L. Gakhar, D. Guilliams, Y. Hao, S. C. Isom, S. Jones, S. Korte, B. Kussman, J. Launspach, M. Linville, E. Mahan, T. Mayhew, C. McHughes, K. Munson, M. Parker, C. Randak, S. Ramachandran, J. Ross, A. Small, L. Spate, D. Vermeer, E. Walters, and J. Whyte for excellent assistance. We thank our patients with CF for inspiration, and we also thank Cystic Fibrosis Foundation Therapeutics and R. Bridges for the gift of GlyH-101. This work was supported by the National Heart Lung and Blood Institute (grant HL51670), the National Institute of Diabetes and Digestive and Kidney Diseases (grant DK54759), Food for the 21st Century, the Cystic Fibrosis Foundation, and HHMI. C.S.R. was supported by NIH training grant HL07638. D.A.S. is a Parker B. Francis Fellow and was supported by the National Institute of Allergy and Infectious Diseases (grant AI076671). M.J.W. is an Investigator of the HHMI. C.S.R., R.S.P., M.J.W., and the University of Iowa Foundation have applied for a patent related to the work reported in this paper, and C.S.R. and M.J.W. are founders of Exemplar Genetics, a company that is licensing materials and technology related to this work. C.S.R. is currently Director of Research and Development at Exemplar Genetics.

Supporting Online Material

www.sciencemag.org/cgi/content/full/321/5897/1837/DC1
Materials and Methods
SOM Text
Figs. S1 to S3
Table S1
References

11 June 2008; accepted 22 August 2008
10.1126/science.1163600

Seeding and Propagation of Untransformed Mouse Mammary Cells in the Lung

Katrina Podsypanina,* Yi-Chieh Nancy Du, Martin Jechlinger, Levi J. Beverly, Dolores Hambardzumyan, Harold Varmus

The acquisition of metastatic ability by tumor cells is considered a late event in the evolution of malignant tumors. We report that untransformed mouse mammary cells that have been engineered to express the inducible oncogenic transgenes MYC and $Kras^{D12}$, or polyoma middle T, and introduced into the systemic circulation of a mouse can bypass transformation at the primary site and develop into metastatic pulmonary lesions upon immediate or delayed oncogene induction. Therefore, previously untransformed mammary cells may establish residence in the lung once they have entered the bloodstream and may assume malignant growth upon oncogene activation. Mammary cells lacking oncogenic transgenes displayed a similar capacity for long-term residence in the lungs but did not form ectopic tumors.

Metastatic dissemination of cancer cells, the major cause of cancer mortality, is traditionally viewed as a late-stage event (*1*), although mammary epithelial cells have been shown to disseminate systemically from early neoplastic lesions in transgenic mice and from ductal carcinoma in situ in women (*2*). There is ample evidence that the ability of fully transformed tumor cells to metastasize depends on the regulation of developmental programs and external environmental cues (*3*–*11*), but to what extent the seeding or growth of tumor cells at the ectopic site is dependent on the initiating transforming event(s) is a subject of debate (*12*). We have developed a system that separates the process of seeding cells in the lung from the process of malignant growth at an ectopic site by using animals engineered to express potent oncogenes in a doxycycline-dependent mammary-specific manner. After intravenous (IV) injection of marked mammary cells that have different genetic potentials [no oncogenes, or oncogenes that will be expressed only after cells have taken up residence in an ectopic site (the lungs)], normal mammary cells can lodge in the lungs, grow slowly, and become frank metastatic malignancies once potent oncogenes are turned on.

We recently described tri-transgenic *TetO-MYC;TetO-Kras^{D12};MMTV-rtTA* (*TOM;TOR;MTB*) mice that coordinately express *MYC* and mutant *Kras* oncogenes in mammary epithelial cells when fed doxycycline (*13*). Doxycycline-naïve animals do not express the transgenic oncogenes and have morphologically and functionally normal mammary glands, but they develop diffuse autochthonous tumors within 3 to 4 weeks after doxycycline exposure. Tumors that form because of the expression of these oncogenes display malignant characteristics, such as transplantability and metastasis (fig. S1). Therefore, this model provides primary mammary cells that can be switched from a normal to a neoplastic state with simple experimental manipulation.

Program in Cancer Biology and Genetics, Memorial Sloan-Kettering Cancer Center, New York, NY 10021, USA.

*To whom correspondence should be addressed. E-mail: podsypak@mskcc.org

Downloaded from www.sciencemag.org on November 6, 2008